Towards earthquake early warning across Europe: Probabilistic quantification of available warning times and their risk-mitigation potential

Gemma Cremen [1], Carmine Galasso[1,2], Elisa Zuccolo[3]

[1]University College London, Department of Civil, Environmental and Geomatic Engineering, London, WC1E 6BT, United Kingdom
[2]Scuola Universitaria Superiore (IUSS) Pavia, Pavia, 27100, Italy
[3]European Centre for Training and Research in Earthquake Engineering (Eucentre), Department of Risk Scenarios, Pavia, 27100, Italy

Key Points:

- EEW feasibility is examined for Europe, considering lead time, alert accuracy, and risk metrics.
- Iceland, Greece, Turkey, and Italy include sites with the highest EEW feasibility.
- EEW could be an effective risk-mitigation tool for a significant portion of Europe.

Corresponding author: Gemma Cremen, g.cremen@ucl.ac.uk

Abstract

We explore the feasibility of implementing earthquake early warning (EEW) across Europe, where there is a clear need to take effective measures for mitigating seismic risk. EEW systems consist of seismic networks and mathematical models/algorithms capable of real-time data telemetry that alert stakeholders (e.g., civil protection authorities and/or the public), to the nucleation of an earthquake seconds/minutes before strong shaking occurs at target sites. During this time, actions can be taken to significantly decrease detrimental impacts. We investigate distributions of EEW warning times available across various parts of the Euro-Mediterranean region, based on seismicity models and seismic network density. We then determine the risk-reduction potential of these times, by defining their spatial relationship with exposure, event-dependent vulnerability, and an alert accuracy proxy, using well-established risk-prediction tools from earthquake engineering. The results are quantitative EEW feasibility maps, which can be used to understand how/if effective European EEW systems can be achieved.

Plain Language Summary

This study examines the potential for using earthquake early warning (EEW) as an effective measure for reducing risks from European earthquakes. EEW systems consist of physical infrastructure and software that can alert stakeholders (e.g., the public and/or civil protection officials) about an incoming earthquake seconds to minutes before they experience the resulting strong shaking. During this time, actions can be taken to significantly decrease the detrimental impacts of the impending shaking. For example, trains can be stopped to avoid derailment, gas supplies can be shut off to prevent fires, and people can take cover to minimise their injury risk. We first investigate the range of EEW warning times available across the parts of the continent that are likely to experience the largest earthquakes. We then determine the potential of these times to reduce risk, by understanding their spatial relationship with people's locations, places that will experience the strongest shaking, and the chances of an alert being correctly received. The results of this study are quantitative maps of EEW feasibility in Europe, which can be used to understand where EEW systems would be effective in the continent and therefore to strategically plan the installation of any future European EEW systems.

1 Introduction

Earthquake early warning (EEW) systems are a relatively recent innovation in earthquake-induced disaster risk reduction and resilience promotion (Allen & Melgar, 2019). They consist of seismic sensor networks and mathematical models/algorithms that are designed to process and disseminate real-time information about ongoing earthquakes. The resulting alert messages enable various stakeholders (e.g., individuals, communities, governments, businesses) located at distance to take timely measures for reducing the likelihood of damage or loss before strong shaking reaches them (UNISDR, 2009). Examples of important risk-mitigation actions that can be taken in the short warning time provided by EEW systems (typically seconds to minutes) include: (1) Performing "drop, cover and hold on" (DCHO) (Porter, 2016) or moving to a safer location (either within a building or outside), to avoid injuries; (2) slowing down high-speed trains, to reduce accidents (Fabozzi et al., 2018); (3) shutting off gas pipelines, to prevent fires (Gasparini et al., 2011); and (4) switching signals to stop vehicles from entering vulnerable infrastructure components (such as bridges), to avoid fatalities (Le Guenan et al., 2016). This list accounts for merely a small number of the vast array of critical applications that can benefit from EEW (Velazquez et al., 2020).

The process of EEW typically involves up to five main steps: (1) Detecting an earthquake, (2) estimating its location; (3) estimating its magnitude; (4) estimating the ground-motion at target sites; and (5) using all of the information collected to decide whether

(or not) to trigger an alarm. EEW systems may be broadly categorised as "regional", "on-site" (or "hybrid"), depending on their approach to the first three steps mentioned above. This study exclusively focuses on regional systems, which consist of seismic station networks installed within the expected epicentral/high seismicity area that record the necessary information for estimating the parameters of Steps 1, 2 and 3. The source parameter estimates of Steps 2 and 3 are then used to predict ground shaking (Step 4) at target sites located further away from the fault rupture (Satriano, Wu, et al., 2011).

Regional EEW systems are presently operating in nine countries (including USA, Mexico, and Japan), and have been tested for application in a further 13 (Cremen & Galasso, 2020). This paper investigates the feasibility of their application in the Euro-Mediterranean area, where there is a strong need to develop effective measures for mitigating seismic risk (Crowley et al., 2018); this is underlined by the fact that the average annual European GDP affected by earthquakes exceeds $20 billion (World Bank, 2017). In addition, the only European countries with current operational EEW systems are Romania (Mârmureanu et al., 2011) and Turkey (Alcik et al., 2009). In particular, we focus on EEW warning time (i.e., the time between the delivery of an EEW alert and the arrival of strong shaking at target sites). We compute probabilistic distributions of warning times available for various seismicity scenarios in high-hazard areas across the continent, using a sophisticated travel-time algorithm incorporating wave propagation physics. We also explicitly quantify the risk-mitigation potential of these times for specific magnitude events, by establishing their spatial relationship with values of proxy measures for seismic vulnerability, exposure, and alert accuracy.

A number of studies have previously explored the feasibility/potential of EEW in different parts of the world, including France (Auclair et al., 2015), Italy (Picozzi, Zollo, et al., 2015; Picozzi, Emolo, et al., 2015; Emolo et al., 2016), Spain (Pazos et al., 2015), Portugal (Oliveira et al., 2015) Turkey (Oth et al., 2010), Japan (Meier et al., 2020), California (Minson et al., 2018, 2019), Hawaii (Thelen et al., 2016), the New Madrid Seismic Zone (Ogweno et al., 2019), and Kyrgyzstan (Picozzi et al., 2013). This work significantly advances the state-of-the-art established by the aforementioned studies for a number of reasons. It examines EEW feasibility on a much larger (i.e., continental level) scale by combining EEW methods, models, and tools in a harmonised framework across Europe. Furthermore, we introduce a novel feasibility metric that enables identification of priority regions for further, more refined EEW feasibility analyses and/or actual investment in EEW systems for targeted end users. This study therefore offers a unique trans-national perspective on the potential of EEW that is highly relevant for intergovernmental stakeholders, such as the International Search and Rescue Advisory Group (INSARAG) of the United Nations (United Nations Office for the Coordination of Humanitarian Affairs, 2015). It also provides valuable new insights on the possible benefits/limitations of EEW for regions (e.g., Iceland and Georgia) that have not recently experienced large earthquakes, but are likely to do so in the future.

2 Methods and Results

2.1 Lead-time mapping for high hazard areas

We focus on crustal point sources associated with large seismic hazard of engineering significance, which we define as those for which the event with a recurrence interval of 500 years is at least M_w 6.5. We use the area source model of the 2013 European Seismic Hazard Model, which accounts for crustal seismicity with depth $\leq$ 40 km (Giardini et al., 2014; Woessner et al., 2015). To define seismic sources, we discretise the model into $0.1^\circ \times 0.1^\circ$ cells. We specifically make use of the depth, maximum magnitude, style-of-faulting, and Gutenberg-Richter a,b parameters from the model. Each source is assumed to be characterised by all parameter values associated with the corresponding area source zone. We use the values associated with the highest weight in the logic tree, where

applicable, and average depth values for stable continental regions. The moment magnitude of the event with a recurrence interval of 500 years for a given source (m) satisfies the following equation:

$$\lambda_m - \lambda_{m_{max}} = 0.002 \tag{1}$$

where λ_m is the annual rate of earthquakes with magnitude greater than m, according to the Gutenberg-Richter magnitude-frequency relationship (de Santis et al., 2011), and m_{max} is the modal maximum magnitude for the given source. We focus on the 37,869 sources for which $m >= 6.5$. The catalog generated to quantify alert accuracy consists of 1,000 eathquakes per source that are Gutenberg-Richter distributed and have uniform annual rates of occurrence (from equation 1) between 0 and 1. Predictions of PGA and and peak ground velocity (PGV) associated with all events are computed/sampled using the epicentral distance version of the Akkar et al. ground motion model (Akkar et al., 2014). The site amplification input to this model is the shear wave velocity in the uppermost 30 m, which is estimated at each target site from a topographic slope map (Wald & Allen, 2007).

For each of these area sources, we calculate potential lead times (i.e., warning times that would be provided by EEW before shaking occurs) at target sites where the predicted median peak ground acceleration (PGA) associated with 500-year recurrence-interval events exceeds 0.05 g, which is a commonly used threshold value for strong earthquake shaking in several engineering applications, including seismic design aimed at life-safety performance (Bolt, 1973; Vanmarcke And & Lai, 1980; Elghazouli, 2016). Seismic station locations are obtained using the IRIS Google map (GMAP) station mapping service (*http://ds.iris.edu/gmap/*). We consider all stations (both temporary and permanent arrays) between $-26°$ and $45°$ longitude, and $34°$ and $72°$ latitude that were in operation until at least the start of 2020. Target sites are equivalent to all land-based seismic sources (i.e. those without a water layer at or above zero-elevation in the corresponding 1-D velocity profile), located within the same coordinate boundaries as the seismic stations. The lead-time (in seconds) for target site j due to an event at a given seismic source a is calculated as follows:

$$LT_j = TT^s_{a,j} - TT^p_{a,st_3} - 4 \tag{2}$$

where $TT^s_{a,j}$ is the S-wave arrival time at j, and TT^p_{a,st_3} is the P-wave arrival time at the third closest station to the source. We account for the triggering of three stations, as it is the minimum required for many popular regional EEW algorithms to report reliable source parameter estimates (Allen et al., 2009; Satriano, Elia, et al., 2011; Cua et al., 2009). A four-second interval is assumed to capture both data telemetry delays and the P-wave window required by an EEW algorithm to compute location/magnitude estimates, in line with previous studies (Picozzi, Zollo, et al., 2015). We use the travel time algorithm of the open-source NonLinLoc software package (*http://alomax.free.fr/nlloc/*) (Lomax et al., 2000). This method calculates first arrival travel times for the nodes of a spatial grid using the Eikonal finite-difference scheme of Podvin and Lecomte (Podvin & Lecomte, 1991), which is an approximation of Huygen's principle (Wagner et al., 2013). We use a grid spacing of 10 km in all directions, and incorporate a normally distributed zero-mean timing error with 0.2 variance. Both source-to-site and source-to-station travel times are calculated using 1-D velocity profiles from the CRUST 1.0 velocity model (Laske et al., 2013), at the location of the target site. Travel times are computed to zero-elevation at the target site.

Figure 1 displays histograms of lead times computed at selected target sites in three major capital cities covered by the study area, i.e., Rome, Istanbul, and Athens, due to the area sources that comply with the previously outlined criteria. It can be seen that the majority of lead times are positive for all three sites. The median lead times for the sites are 4.0 seconds (Rome), 6.5 seconds (Istanbul), and 5.8 seconds (Athens), while the standard deviations of the times (in the same order) are 3.6, 5.7, and 5.0; these uncer-

166 tainties are significant, reflecting the large variation in source-to-site distances for a given
site.

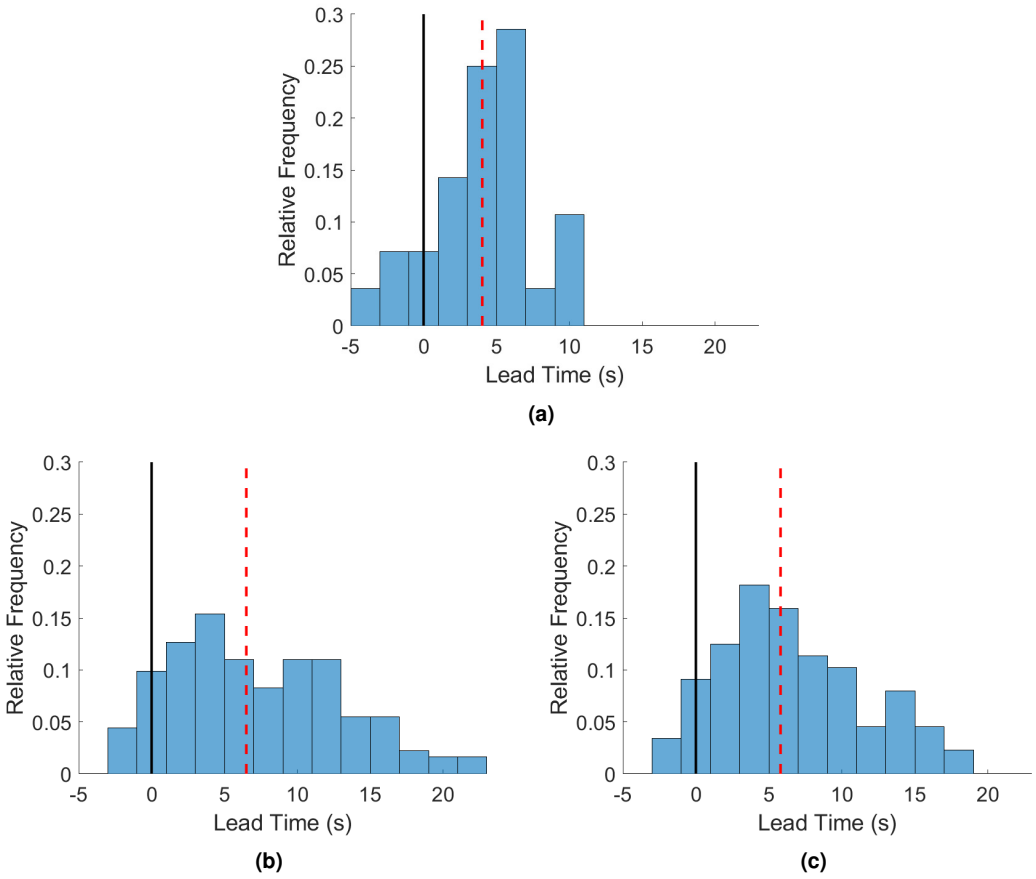

Figure 1. Distributions of lead times for target sites in three major European capital cities. (a) Site in Rome, (b) site in Istanbul, and (c) site in Athens. Note that the red dashed lines indicate the corresponding median lead times and the black solid lines denote the positive lead-time threshold.

167

168 Figure 2 contains maps displaying the following three summary statistics for all af-
169 fected target sites across the continent: (1) minimum lead time (i.e., "worst case scenario");
170 (2) median lead time; and (3) maximum lead time (i.e., "best case scenario"). Also pro-
171 vided is a summary of potential risk-reducing actions that can be carried out for the var-
172 ious ranges of lead time investigated. Note that negative lead times correspond to blind
173 zones, where no warning is received before strong shaking occurs. Of all target sites ex-
174 amined, 7% have positive minimum lead times (<1% greater than 10 seconds, 2% be-
175 tween 5 and 10 seconds, and 5% less than 5 seconds); 46% have positive median lead times
176 (2% greater than 10 seconds, 9% between 5 and 10 seconds, and 35% less than 5 seconds);
177 and 91% have positive maximum lead times (44% greater than 10 seconds, 30% between

5 and 10 seconds, and 17% less than 5 seconds). The maximum lead time achieved across all target sites examined is 34.0 seconds (near Bafra, northern Turkey). Countries containing target sites with the longest overall lead times are Iceland, Greece and Turkey, which are characterised by some of the strongest seismicity in Europe. On the other hand, countries containing target sites with the shortest overall lead times are Iraq, Georgia, and Russia.

We verify the adequacy of the resolution chosen for the lead-time map, by benchmarking the resulting times for Italy with those obtained using area source zones discretised into 0.05°×0.05° cells, which is equivalent to the resolution used in the country's official seismic hazard map (Stucchi et al., 2004). There are no notable differences in the lead times obtained at both resolutions. Therefore, the grid spacing of the European-wide map is deemed adequate.

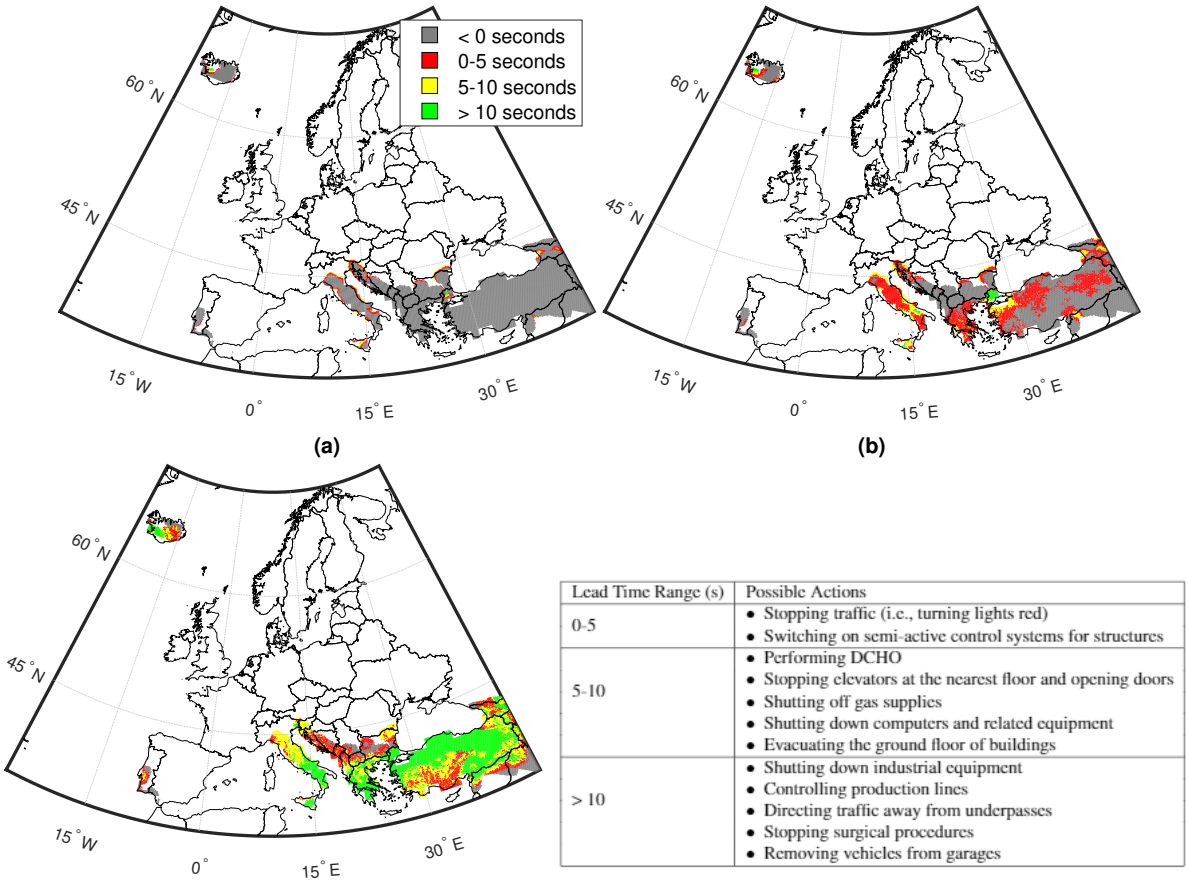

Lead Time Range (s)	Possible Actions
0-5	• Stopping traffic (i.e., turning lights red) • Switching on semi-active control systems for structures
5-10	• Performing DCHO • Stopping elevators at the nearest floor and opening doors • Shutting off gas supplies • Shutting down computers and related equipment • Evacuating the ground floor of buildings
> 10	• Shutting down industrial equipment • Controlling production lines • Directing traffic away from underpasses • Stopping surgical procedures • Removing vehicles from garages

Figure 2. Lead-time mapping across all examined target sites. (a) Minimum lead times (b) median lead times, and (c) maximum lead times. (d) Details the possible risk-mitigation actions that can be taken by various stakeholders for different lengths of EEW lead time, adapted from previous work (Iervolino, 2011; James D. Goltz, 2002; Porter, 2016; Iervolino, Galasso, & Manfredi, 2007; Oliveira et al., 2015).

2.2 Risk Quantification

We examine the risk-mitigation potential of the calculated lead times, by defining their spatial relationship with ambient (average day/night) population distributions and

the average seismic intensity across all events with a recurrence interval of 500 years that produce a PGA greater than or equal to 0.05 g at the affected site. Seismic intensities are calculated from the bilinear equations for EMS-98 macroseismic intensity developed by Masi et al. (Masi et al., 2020), using the PGV predictions discussed in Section 2.1. Population data are obtained from the 2018 LandScan database (Rose et al., 2019), which contains global ambient population distributions at a $30'' \times 30''$ spatial resolution. Each target site is assigned the aggregated population across all LandScan grid points closest to it.

Population is an important consideration in seismic risk assessment (Tenerelli et al., 2015) that often acts as a proxy for the exposure (i.e., the value at risk) of the built environment/assets in earthquake engineering and risk modelling applications (Ceferino et al., 2018). Seismic intensity, which describes the effect of earthquake ground shaking on the built environment and communities, is a well-established proxy for both damage (Wald et al., 1999) and vulnerability (Grunthal & European Seismological Commission. Working Group "Macroseismic Scales.", 1998). We use the EMS-98 seismic intensity scale (Grunthal & European Seismological Commission. Working Group "Macroseismic Scales.", 1998), which is specifically designed for European countries.

98% of the total ambient population surrounding the examined target sites are affected by average EMS-98 values between V ("Strong" e.g., top-heavy objects topple over) and VII ("Damaging" e.g., many objects fall from shelves and there is some wall damage). Figure 3 indicates that approximately 38% of the ambient population are affected by EMS-98 values between V and VI ("Slightly damaging" e.g., objects fall from walls and there is some damage to plaster), while approximately 60% are affected by values between VI and VII. 38% of the ambient population affected by average intensities between V and VI have maximum lead times greater than 10 seconds, while 10% have negative maximum lead times (i.e., they are located in the "blind zone"). 59% of this population have positive median lead times, and 18% have positive minimum lead times. 65% of the ambient population affected by average intensities between VI and VII have maximum lead times greater than 10 seconds, while 4% are located in the "blind zone". 56% of this population have positive median lead times, and 1% have positive minimum lead times.

2.2.1 EEW feasibility calculation

For a given target site j, we combine estimates of median lead-time (L), average seismic intensity (I), and affected ambient population (P) into a single novel metric of EEW feasibility, termed the EEW Relative Feasibility Index (RF_j). RF_j is defined as follows:

$$RF_j = F_L(L_j) \times w_L + F_I(i_j) \times w_I + F_P(p_j) \times w_P \tag{3}$$

where $F_X(x_k)$ is the empirical cumulative distribution function of X (across all examined target sites with positive median lead time) evaluated at k, and w_X is the stakeholder-assigned weight for X (note that $w_P + w_I + w_L = 1$). Higher values of this index correspond to key characteristics that maximise the effectiveness of an EEW system (Kuyuk & Allen, 2013), i.e.: (1) longer lead times; (2) higher potential for shaking causing losses that can be avoided with EEW; and (3) larger affected populations. They therefore indicate greater EEW feasibility for a given target site.

It can be seen from equation 3 that the index accommodates a user-defined weight for each measurement, to account for stakeholder preferences and priorities. Figure 4 includes EEW Relative Feasibility Index mapping of all target sites with positive median lead time, for the equally-weighted case (i.e., $w_P = w_I = w_L = 0.333$) and for cases where one variable (e.g., lead time) is weighted three times more than the other two (e.g., $w_L = 0.6$, and $w_P = w_I = 0.2$). Also highlighted in each subplot are the fifty target sites with the largest index values for the corresponding case.

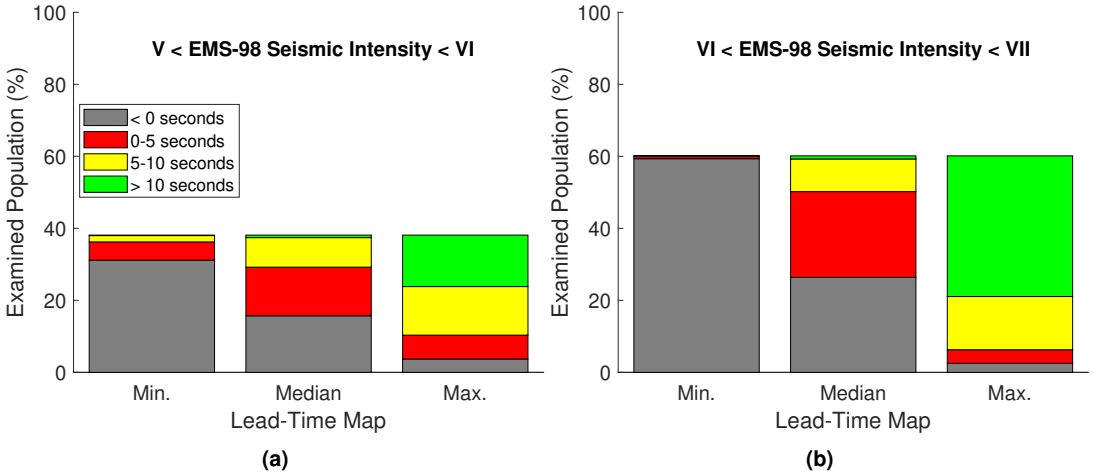

Figure 3. Examining the risk-mitigation potential of calculated lead times. Average EMS-98 macroseismic intensities experienced by the affected ambient population during events with a recurrence interval of 500 years that resulted in at least 0.05 g PGA at the associated target site, categorised by the corresponding times of the maps presented in Figure 2. Note that seismic intensities V, VI, and VII denote "strong", "slightly damaging", and "damaging" events, respectively.

For all cases, the countries containing sites with the fifty largest feasibility indices are Italy, Turkey, and Greece. However, both the locations and the number of sites per country differ between cases. Relative to the equally weighted case, target sites with the largest increase and decrease in feasibility index for the case where lead time is the most weighted variable are located in Iceland and Turkey respectively, target sites with the largest increase and decrease in this value for the case where seismic intensity is the most weighted variable are located in Turkey and Georgia respectively, and target sites with the largest increase and decrease in feasibility index for the case where population is the most weighted variable are both located in Turkey.

Finally, we investigate the impact of alert accuracy (i.e., the ability of the system not to miss or provide false warnings) on EEW feasibility. We specifically adopt the approach of Minson et al. (Minson et al., 2019), which examines the forecasting capability of EEW in terms of ground motion prediction accuracy for a set of known source parameters. We randomly sample PGA values at each site for a series of earthquakes across nearby sources, assuming that an alert is issued if the corresponding median predicted PGA exceeds 0.05 g. The relative feasibility indices of Figure 4a are then scaled by the relative proportion of correctly issued alerts to produce Figure 4e, according to:

$$RF_{j,alert} = RF_j \times F_{CA}(ca_j) \tag{4}$$

where ca_j is the proportion of correct alerts at site j, calculated as:

$$ca_j = \frac{n_{ca,j}}{n_j} \tag{5}$$

n_j is the total number of catalog earthquakes examined for j, which is all events from sources considered in the lead-time calculation that yield a predicted median PGA at

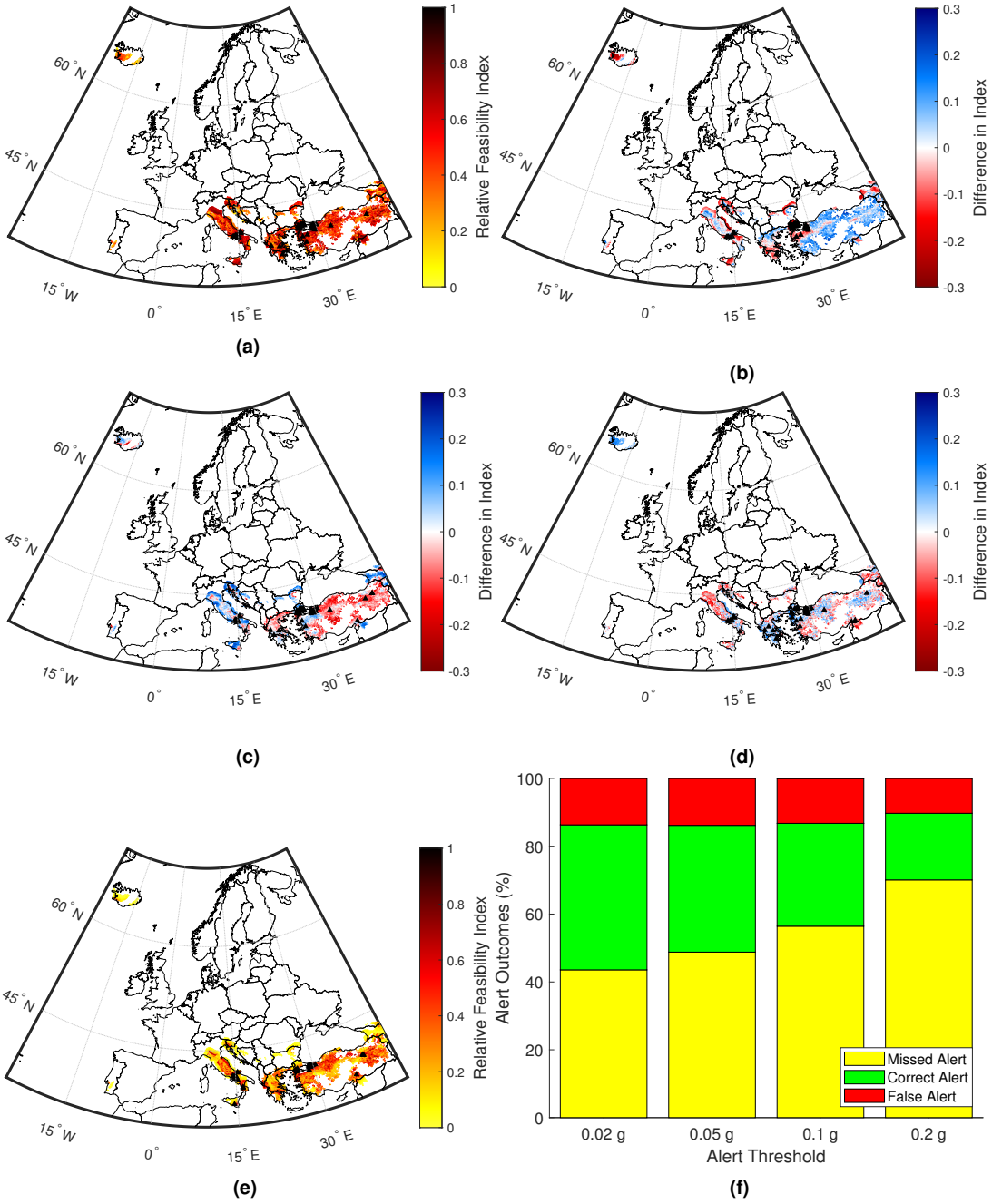

Figure 4. Relative Feasibility Index mapping across examined target sites. Indices for (a) the case in which lead time, intensity, and population are equally weighted by a stakeholder, as well as differences for cases in which (b) lead time, (c) seismic intensity, and (d) population are respectively weighted three times more than both other variables. Also shown are (e) equally weighted indices scaled by the relative number of correctly issued alerts (for 0.05 g alert threshold) and (f) the proportion of different alert outcomes across all of the thresholds examined in (Minson et al., 2019). Note that for (b)-(d), red colours indicate an increase in the index relative to (a) and blue colours indicate a relative decrease. Black triangles indicate target sites with one of the fifty largest indices for each case.

the site of at least 0.001 g and result in either a false alert, a missed alert, or a correct alert ($n_{CA,j}$) - we ignore cases where the system correctly issues no alert, in line with Minson et al (Minson et al., 2019). A false alert occurs if the predicted median PGA exceeds the threshold and the actual (randomly simulated) PGA does not, while a missed alert occurs in the opposite case. All other considered combinations of predicted median and actual ground shaking produce a correct alert.

It can be seen that alert accuracy has a significantly detrimental effect on the feasibility of some target sites, reducing indices by up to approximately 0.8. It causes the smallest and largest feasibility decreases in Slovenia and Turkey, respectively. However, target sites with the largest feasibility are still located in Italy, Turkey, and Greece (along with Iceland). It is important to note that alert accuracy is highly dependent on the selected threshold. To demonstrate this, Figure 4f shows a summary of the proportion of different alert outcomes obtained across all sites considered in this study, as a function of the various alert thresholds examined in Minson et al. (Minson et al., 2019). In particular, it can be seen that the number of correct alerts decreases with increasing threshold. This trend was also observed for California data by Minson et al, who obtained similar alert outcome proportions to those in Figure 4f.

Discussion

This study has examined the feasibility of EEW for Euro-Mediterranean regions affected by significant seismic hazard. Probabilistic distributions of EEW lead (warning) times were determined for target sites in these areas, by randomly varying the location of seismic sources in line with regional seismicity. Summary statistics of these times were then translated into maps, which give additional promising indications of the potential usefulness of EEW in Europe. For example, they show that almost half (i.e., 44%) of the examined target sites benefit from warning times greater than 10 seconds in a "best case scenario" that are long enough to accommodate major risk intervention actions, such as the shutting down of industrial equipment or the removal of vehicles from garages. 11% of all examined target sites have a 50% chance of receiving an EEW alert greater than 5 seconds ahead of shaking that at least allows time for people to "drop, cover and hold on", shut off gas supplies, or evacuate ground floors in buildings. Even in a "worst case scenario", more than 5% of target sites have enough warning time (up to 5 seconds) for the switching on of semi-active control systems in structures (Maddaloni et al., 2011), which could significantly reduce structural vulnerability and resulting damage/loss. We found that the longest overall lead times occur at sites in Iceland, Greece, and Turkey. Areas associated with the shortest overall lead times, and therefore where the feasibility of EEW could be particularly improved through increased seismic station density, are northern Iraq, north-western Georgia, and southern Russia.

We further contextualised the significance of the lead times by combining them with spatial distributions of two risk proxies often used in earthquake engineering (i.e., population and seismic intensity). We found that almost all (i.e, approximately 98%) of the affected ambient population are exposed to average seismic intensities from nearby seismic sources that at least result in some falling objects. More than 50% of these people have greater than 10 seconds of warning time in a "best case scenario", which enables them to carry out the major risk intervention actions mentioned in the previous paragraph. A significant proportion ($> 55\%$) have positive warning times from events at 50% of relevant sources, while approximately 8% have some warning time in a "worst case scenario".

Finally, we translated the aforementioned features (i.e., (1) lead time; (2) average seismic intensity from nearby sources; and (3) ambient population affected) into a novel indicator for measuring relative EEW feasibility at a given target site that also accounts for stakeholder-specific preferences. A corresponding feasibility map was developed for

the case in which the features were equally weighted, as well as cases where each feature was weighted three times more than the other two. While there was some variation in the results obtained for different weighting strategies, all maps indicated that Turkey, Italy, and Greece contain the target sites with the highest EEW feasibility. We additionally examined the impact of alert accuracy on the equally weighted feasibility map, and found that Turkey, Italy, and Greece still demonstrated the highest feasibility (along with Iceland). The indices of some target sites were significantly reduced (by up to almost 90%) in this case. However, this outcome is highly dependent on the assumed alert threshold (i.e., 0.05 g) (Minson et al., 2019). Using an alternative threshold of 0.02 g, for example, would have increased the accuracy of the worst-performing source-site combination by more than 20 times, due to less missed alerts. Note that in reality, the optimal threshold will be application-specific, depending on structural characteristics at the target site (Iervolino, Giorgio, & Manfredi, 2007) as well as stakeholder preferences/tolerances towards risk(Le Guenan et al., 2016).

The findings of this study suggest that an expansion/enhancement of Istanbul-focused EEW efforts could be significantly beneficial for mitigating seismic risk in many regions throughout Turkey. The results are particularly notable for Italy and Greece, since neither has a currently operational EEW system. In summary, we ultimately conclude that this work provides strong evidence to suggest that EEW could be an effective tool for supporting earthquake-related disaster risk reduction across a significant proportion of Europe. A new three-year Horizon 2020 European research project called TURNkey (*Towards more Earthquake-resilient Urban Societies through a Multi-sensor-based Information System enabling Earthquake Forecasting, Early Warning and Rapid Response actions*; see **Acknowledgements** section) aims to address this issue by developing a holistic earthquake information system that incorporates state-of-the-art seismic risk mitigation tools for both operational earthquake forecasting and EEW in real- and near-real time, with selected testbeds in Italy and Greece (as well as Iceland) to be the focus of more detailed analyses for EEW and the target of end-user-orientated applications of the system.

It is important to note that there are some limitations/simplifying assumptions associated with this work. Firstly, it is assumed that the seismic stations currently installed across the Euro-Mediterranean area (both permanent and temporary) are capable of being used for early warning purposes (i.e., they have adequate data acquisition/transmission systems, real-time communication capability, robust dissemination methods, power supply systems, etc. (Auclair et al., 2015; Thelen et al., 2016)), which may be an over-simplification (Allen & Melgar, 2019). We did not explicitly consider the performance of existing EEW algorithms in the lead-time calculations. Instead, we simply assumed that four seconds was sufficient to capture both data telemetry delays and the length of time required by the algorithms to estimate relevant source parameters (see Section 2.1); a slightly longer time ($\sim$ five seconds) may be required for certain algorithms and transmission features (Allen, 2007; Behr et al., 2015). Our detailed EEW feasibility analysis only accounted for crustal seismic sources, thereby yielding conservative lead times for target sites that would additionally be affected by the deeper seismicity of subduction zones in the Central and Eastern Mediterranean Sea. It therefore also neglected the seismicity of the Vrancea region in Romania (Ismail-Zadeh et al., 2012), which has significant associated hazard (Sokolov et al., 2009); examination of this region is not crucial in the context of our study however, given that it already has an operational EEW system (Mârmureanu et al., 2011; Ionescu et al., 2007). To maintain a consistent approach for the entire examined region, the considered seismicity scenarios were defined using an area source model (see Section 2.1), which assumes a uniform occurrence of earthquakes as point sources; thus, the resulting calculations of hazard near faults (large seismogenic sources) may not be completely realistic (Valentini et al., 2017). Our approach to quantifying alert accuracy only considered the variability of a ground motion model (Minson et al., 2019). Precisely characterising warning accuracy would involve more detailed analysis with the specific al-

gorithms of operational EEW platforms, including the quantification and propagation of uncertainties at each step of the calculations. This type of examination was carried out for select testbed sites across Europe in a previous study by the same authors (Zuccolo et al., 2020). It is outside the scope of this paper, given the continent-wide extent of the study. Finally, we did not consider the economic value of EEW, i.e., the costs required to build and maintain EEW systems compared to the monetary savings they provide through avoided damage (Klafft & Meissen, 2011). Despite these constraints, this study nevertheless represents an innovative attempt to comprehensively quantify EEW feasibility on a continental scale and to identify priority regions for more detailed EEW feasibility analyses/investment in EEW implementation.

Acknowledgments

We obtained seismic station locations from the IRIS Google map (GMAP) station mapping service (*http://ds.iris.edu/gmap/*). Seismic source data and general target site locations were retrieved from the 2013 European Seismic Hazard Model (Giardini et al., 2014; Woessner et al., 2015). We determined target sites for the Italian benchmarking study using the 'Countries WGS84' shapefile in the ArcGIS Hub (*https://hub.arcgis.com/search*). We obtained estimates of shear wave velocity in the uppermost 30 m from the database of Wald and Allen (2007). Velocity profiles were acquired from the CRUST 1.0 dataset (Laske et al., 2013). Population data were obtained from the 2018 Landscan database (Rose et al., 2019).

We thank Dr. Alireza Azarbakht and Dr. John Douglas (University of Strathclyde, UK) for helpful feedback on parts of this study. This paper is supported by the European Union's Horizon 2020 research and innovation programme under grant agreement No 821046, project TURNkey (Towards more Earthquake-resilient Urban Societies through a Multi-sensor-based Information System enabling Earthquake Forecasting, Early Warning and Rapid Response actions; *https://earthquake-turnkey.eu/*.

References

Akkar, S., Sandıkkaya, M. A., & Bommer, J. J. (2014). Empirical ground-motion models for point- and extended-source crustal earthquake scenarios in Europe and the Middle East. *Bulletin of Earthquake Engineering*, *12*(1), 359–387. doi: 10.1007/s10518-013-9461-4

Alcik, H., Ozel, O., Apaydin, N., & Erdik, M. (2009, 3). A study on warning algorithms for Istanbul earthquake early warning system. *Geophysical Research Letters*, *36*(5). doi: 10.1029/2008GL036659

Allen, R. M. (2007). The elarms earthquake early warning methodology and application across california. In *Earthquake early warning systems* (pp. 21–43). Springer.

Allen, R. M., Brown, H., Hellweg, M., Khainovski, O., Lombard, P., & Neuhauser, D. (2009, 3). Real-time earthquake detection and hazard assessment by ElarmS across California. *Geophysical Research Letters*, *36*(5). doi: 10.1029/2008GL036766

Allen, R. M., & Melgar, D. (2019). Earthquake Early Warning: Advances, Scientific Challenges, and Societal Needs. *Annual Review of Earth and Planetary Sciences*, *47*. Retrieved from `https://doi.org/10.1146/annurev-earth-053018-` doi: 10.1146/annurev-earth-053018

Auclair, S., Goula, X., Jara, J. A., & Colom, Y. (2015, 9). Feasibility and Interest in Earthquake Early Warning Systems for Areas of Moderate Seismicity: Case Study for the Pyrenees. *Pure and Applied Geophysics*, *172*(9), 2449–2465. doi: 10.1007/s00024-014-0957-x

Behr, Y., Clinton, J., Kästli, P., Cauzzi, C., Racine, R., & Meier, M.-A. (2015). Anatomy of an earthquake early warning (eew) alert: Predicting time delays for an end-to-end eew system. *Seismol. Res. Lett*, *86*(3), 830–840.

Bolt, B. (1973). Duration Of Strong Motion. In *5th world conference on earthquake engineering.* Rome.

Ceferino, L., Kiremidjian, A., & Deierlein, G. (2018, 11). *Regional multiseverity casualty estimation due to building damage following a Mw 8.8 Earthquake Scenario in Lima, Peru* (Vol. 34) (No. 4). Earthquake Engineering Research Institute. doi: 10.1193/080617EQS154M

Cremen, G., & Galasso, C. (2020). Earthquake early warning: Recent advances and perspectives. *Earth-Science Reviews*, 103184.

Crowley, H., Rodrigues, D., Silva, V., Despotaki, V., Romão, X., Castro, J. M., ... Wenzel, M. (2018). TOWARDS A UNIFORM EARTHQUAKE RISK MODEL FOR EUROPE. In *16th european conference on earthquake engineering.* Thessaloniki. Retrieved from `http://www.sera-eu.org/en/activities/joint-research/`

Cua, G., Fischer, M., Heaton, T., & Wiemer, S. (2009, 9). Real-time performance of the virtual seismologist earthquake early warning algorithm in Southern California. *Seismological Research Letters*, *80*(5), 740–747. doi: 10.1785/gssrl.80.5.740

de Santis, A., Cianchini, G., Favali, P., Beranzoli, L., & Boschi, E. (2011, 6). The Gutenberg-Richter law and entropy of earthquakes: Two case studies in central Italy. *Bulletin of the Seismological Society of America*, *101*(3), 1386–1395. doi: 10.1785/0120090390

Elghazouli, A. Y. (2016). *Seismic Design of Buildings to Eurocode 8.* Boca Raton: CRC Press, Taylor & Francis Group.

Emolo, A., Picozzi, M., Festa, G., Martino, C., Colombelli, S., Caruso, A., ... Miranda, N. (2016, 9). Earthquake early warning feasibility in the Campania region (southern Italy) and demonstration system for public school buildings. *Bulletin of Earthquake Engineering*, *14*(9), 2513–2529. doi: 10.1007/s10518-016-9865-z

Fabozzi, S., Bilotta, E., Picozzi, M., & Zollo, A. (2018, 9). Feasibility study of a loss-driven earthquake early warning and rapid response systems for tunnels of the Italian high-speed railway network. *Soil Dynamics and Earthquake Engineering*, *112*, 232–242. doi: 10.1016/j.soildyn.2018.05.019

Gasparini, P., Manfredi, G., & Zschau, J. (2011). Earthquake early warning as a tool for improving society's resilience and crisis response. *Soil Dynamics and Earthquake Engineering*. doi: 10.1016/j.soildyn.2010.09.004

Giardini, D., Wössner, J., & Danciu, L. (2014). Mapping Europe's Seismic Hazard. *TRANSACTIONS*, *95*(29), 261–268. doi: 10.12686/SED

Grunthal, G., & European Seismological Commission. Working Group "Macroseismic Scales.". (1998). *European macroseismic scale 1998 : EMS-98.* European Seismological Commission, Subcommission on Engineering Seismology, Working Group Macroseismic scales.

Iervolino, I. (2011, 2). Performance-based earthquake early warning. *Soil Dynamics and Earthquake Engineering*, *31*(2), 209–222. doi: 10.1016/j.soildyn.2010.07.010

Iervolino, I., Galasso, C., & Manfredi, G. (2007). Information-dependent lead-time maps for earthquake early warning in the Campania region. In *14th world conference on earthquake engineering.* Beijing. Retrieved from `http://www.rissclab.unina.it`

Iervolino, I., Giorgio, M., & Manfredi, G. (2007, 7). Expected loss-based alarm threshold set for earthquake early warning systems. *Earthquake Engineering and Structural Dynamics*, *36*(9), 1151–1168. doi: 10.1002/eqe.675

Ionescu, C., Bose, M., Wenzel, F., Marmureanu, A., Grigore, A., & Marmureanu, G.

(2007). An early warning system for deep Vrancea (Romania) earthquakes. In *Earthquake early warning systems* (pp. 343–349). Springer.

Ismail-Zadeh, A., Matenco, L., Radulian, M., Cloetingh, S., & Panza, G. (2012). *Geodynamics and intermediate-depth seismicity in Vrancea (the south-eastern Carpathians): Current state-of-the art.* doi: 10.1016/j.tecto.2012.01.016

James D. Goltz. (2002). *Introducing earthquake early warning in California - A summary of social science and public policy issues* (Tech. Rep.). Pasadena, California: Governor's Office of Emergency Services.

Klafft, M., & Meissen, U. (2011). Assessing the Economic Value of Early Warning Systems. In *Proceedings of the 8th international conference on information systems for crisis response and management,*. Lisbon. Retrieved from `https://www.researchgate.net/publication/228269557`

Kuyuk, H. S., & Allen, R. M. (2013, 11). Optimal seismic network density for earthquake early warning: A case study from California. *Seismological Research Letters*, *84*(6), 946–954. doi: 10.1785/0220130043

Laske, G., Masters, G., Ma, Z., & Pasyanos, M. (2013). Update on CRUST1.0 - A 1-degree global model of Earth's crust. *Geophysical Research Abstracts*, *15*(EGU2013-2658).

Le Guenan, T., Smai, F., Loschetter, A., Auclair, S., Monfort, D., Taillefer, N., & Douglas, J. (2016, 1). Accounting for end-user preferences in earthquake early warning systems. *Bulletin of Earthquake Engineering*, *14*(1), 297–319. doi: 10.1007/s10518-015-9802-6

Lomax, A., Virieux, J., Volant, P., & Berge-Thierry, C. (2000). Probabilistic Earthquake Location in 3D and Layered Models. In *Advances in seismic event location.* Springer, Dordrecht.

Maddaloni, G., Caterino, N., & Occhiuzzi, A. (2011, 10). Semi-active control of the benchmark highway bridge based on seismic early warning systems. *Bulletin of Earthquake Engineering*, *9*(5), 1703–1715. doi: 10.1007/s10518-011-9259-1

Mârmureanu, A., Ionescu, C., & Cioflan, C. O. (2011). Advanced real-time acquisition of the Vrancea earthquake early warning system. *Soil Dynamics and Earthquake Engineering*. doi: 10.1016/j.soildyn.2010.10.002

Masi, A., Chiauzzi, L., Nicodemo, G., & Manfredi, V. (2020, 3). Correlations between macroseismic intensity estimations and ground motion measures of seismic events. *Bulletin of Earthquake Engineering*, *18*(5), 1899–1932. doi: 10.1007/s10518-019-00782-2

Meier, M. A., Kodera, Y., Böse, M., Chung, A., Hoshiba, M., Cochran, E., ... Heaton, T. (2020, 2). How Often Can Earthquake Early Warning Systems Alert Sites With High-Intensity Ground Motion? *Journal of Geophysical Research: Solid Earth*, *125*(2). doi: 10.1029/2019JB017718

Minson, S. E., Baltay, A. S., Cochran, E. S., Hanks, T. C., Page, M. T., McBride, S. K., ... Meier, M. A. (2019, 12). The Limits of Earthquake Early Warning Accuracy and Best Alerting Strategy. *Scientific Reports*, *9*(1). doi: 10.1038/s41598-019-39384-y

Minson, S. E., Meier, M.-A., Baltay, A. S., Hanks, T. C., & Cochran, E. S. (2018). The limits of earthquake early warning: Timeliness of ground motion estimates. *Science Advances*, *4*(3). Retrieved from `http://advances.sciencemag.org/`

Ogweno, L. P., Withers, M. M., & Cramer, C. H. (2019). Earthquake Early Warning Feasibility Study for the New Madrid Seismic Zone. *Seismological Research Letters*, *90*(3), 1377–1392.

Oliveira, C. S., Mota de Sá, F., Lopes, M., Ferreira, M. A., & Pais, I. (2015, 9). Early Warning Systems: Feasibility and End-Users' Point of View. *Pure and Applied Geophysics*, *172*(9), 2353–2370. doi: 10.1007/s00024-014-0999-0

Oth, A., Böse, M., Wenzel, F., Köhler, N., & Erdik, M. (2010). Evaluation and optimization of seismic networks and algorithms for earthquake early

warning-the case of Istanbul (Turkey). *J. Geophys. Res*, *115*, 10311. doi: 10.1029/2010JB007447

Pazos, A., Romeu, N., Lozano, L., Colom, Y., López Mesa, M., Goula, X., ... Carrilho, F. (2015, 4). A regional approach for earthquake early warning in South West Iberia: A feasibility study. *Bulletin of the Seismological Society of America*, *105*(2), 560–567. doi: 10.1785/0120140101

Picozzi, M., Bindi, D., Pittore, M., Kieling, K., & Parolai, S. (2013). Real-time risk assessment in seismic early warning and rapid response: A feasibility study in Bishkek (Kyrgyzstan). *Journal of Seismology*, *17*(2), 485–505. doi: 10.1007/s10950-012-9332-5

Picozzi, M., Emolo, A., Martino, C., Zollo, A., Miranda, N., Verderame, G., ... Amelia, A. (2015, 3). Earthquake early warning system for schools: A feasibility study in southern Italy. *Seismological Research Letters*, *86*(2A), 398–412. doi: 10.1785/0220140194

Picozzi, M., Zollo, A., Brondi, P., Colombelli, S., Elia, L., & Martino, C. (2015, 4). Exploring the feasibility of a nationwide earthquake early warning system in Italy. *Journal of Geophysical Research: Solid Earth*, *120*(4), 2446–2465. doi: 10.1002/2014JB011669

Podvin, P., & Lecomte, I. (1991). Finite difference computation of traveltimes in very contrasted velocity models: a massively parallel approach and its associated tools. *Geophysics Journal International*, *105*, 271–284. Retrieved from `https://academic.oup.com/gji/article-abstract/105/1/271/671376`

Porter, K. A. (2016). *How Many Injuries can be Avoided through Earthquake Early Warning and Drop, Cover, and Hold On?* (Tech. Rep.). Boulder, Colorado: Structural Engineering and Structural Mechanics Program, Department of Civil Environmental and Architectural Engineering,University of Colorado, Boulder.

Rose, A. N., McKee, J. J., Urban, M. L., & Bright, E. A. (2019). *LandScan 2018.* Oak Ridge, TN: Oak Ridge National Laboratory.

Satriano, C., Elia, L., Martino, C., Lancieri, M., Zollo, A., & Iannaccone, G. (2011, 2). PRESTo, the earthquake early warning system for Southern Italy: Concepts, capabilities and future perspectives. *Soil Dynamics and Earthquake Engineering*, *31*(2), 137–153. doi: 10.1016/j.soildyn.2010.06.008

Satriano, C., Wu, Y. M., Zollo, A., & Kanamori, H. (2011, 2). Earthquake early warning: Concepts, methods and physical grounds. *Soil Dynamics and Earthquake Engineering*, *31*(2), 106–118. doi: 10.1016/j.soildyn.2010.07.007

Sokolov, V. Y., Wenzel, F., & Mohindra, R. (2009). Probabilistic seismic hazard assessment for Romania and sensitivity analysis: A case of joint consideration of intermediate-depth (Vrancea) and shallow (crustal) seismicity. *Soil Dynamics and Earthquake Engineering*. doi: 10.1016/j.soildyn.2008.04.004

Stucchi, M., Meletti, C., Montaldo, V., Akinci, A., Faccioli, E., Gasperini, P., ... Valensise, G. (2004). *Pericolosità sismica di riferimento per il territorio nazionale MPS04 [Data set].* Istituto Nazionale di Geofisica e Vulcanologia (INGV). doi: https://doi.org/10.13127/sh/mps04/ag

Tenerelli, P., Gallego, J. F., & Ehrlich, D. (2015). Population density modelling in support of disaster risk assessment. *International Journal of Disaster Risk Reduction*. doi: 10.1016/j.ijdrr.2015.07.015

Thelen, W. A., Hotovec-Ellis, A. J., & Bodin, P. (2016). *Feasibility Study of Earthquake Early Warning (EEW) in Hawaii. Open-File Report 2016-1172* (Tech. Rep.). U.S. Geological Survey.

UNISDR. (2009). *2009 UNISDR Terminology on Disaster Risk Reduction* (Tech. Rep.). Geneva, Switzerland: UN International Strategy for Disaster Risk Reduction (UNISDR). Retrieved from `www.preventionweb.net`

United Nations Office for the Coordination of Humanitarian Affairs. (2015). *INSARAG Guidelines V1, Policy* (Tech. Rep.). United Nations.

Valentini, A., Visini, F., & Pace, B. (2017, 11). Integrating faults and past earthquakes into a probabilistic seismic hazard model for peninsular Italy. *Natural Hazards and Earth System Sciences*, *17*(11), 2017–2039. doi: 10.5194/nhess-17-2017-2017

Vanmarcke And, E. H., & Lai, S.-S. P. (1980). Strong-motion duration and RMS amplitude of earthquake records. *Bulletin of the Seismological Society of America*, *70*(4), 1293–1307. Retrieved from `https://pubs.geoscienceworld.org/ssa/bssa/article-pdf/70/4/1293/2703468/BSSA0700041293.pdf`

Velazquez, O., Pescaroli, G., Cremen, G., & Galasso, C. (2020). A review of the technical and socio-organisational components of earthquake early warning systems. *Frontiers in Earth Science*, *(in press)*.

Wagner, M., Husen, S., Lomax, A., Kissling, E., & Giardini, D. (2013, 5). High-precision earthquake locations in switzerland using regional secondary arrivals in a 3-D velocity model. *Geophysical Journal International*, *193*(3), 1589–1607. doi: 10.1093/gji/ggt052

Wald, D. J., & Allen, T. (2007, 10). *Topographic slope as a proxy for seismic site conditions and amplification* (Vol. 97) (No. 5). doi: 10.1785/0120060267

Wald, D. J., Quitoriano, V., Heaton, T. H., & Kanamori, H. (1999). Relationships between peak ground acceleration, peak ground velocity, and modified mercalli intensity in california. *Earthquake spectra*, *15*(3), 557–564.

Woessner, J., Laurentiu, D., Giardini, D., Crowley, H., Cotton, F., Grünthal, G., ... Stucchi, M. (2015, 12). The 2013 European Seismic Hazard Model: key components and results. *Bulletin of Earthquake Engineering*, *13*(12), 3553–3596. doi: 10.1007/s10518-015-9795-1

World Bank. (2017). *Europe and Central Asia - Country risk profiles for floods and earthquakes (English)* (Tech. Rep.). Washington, D.C.: World Bank Group.

Zuccolo, E., Cremen, G., Galasso, C., & Roessler, D. (2020). Comparing the performance of regional earthquake early warning algorithms in europe. *Earth and Space Science Open Archive*.